Uncertainty in the ENSO amplitude change from the past to the future

Masahiro Watanabe,[1] Jong-Seong Kug,[2] Fei-Fei Jin,[3] Mat Collins,[4,5] Masamichi Ohba,[6] and Andrew T. Wittenberg[7]

Received 26 July 2012; revised 10 September 2012; accepted 16 September 2012; published 17 October 2012.

[1] Due to errors in complex coupled feedbacks that compensate differently in different global climate models, as well as nonlinear nature of El Niño-Southern Oscillation (ENSO), there remain difficulties in detecting and evaluating the reason for the past and future changes in the ENSO amplitude, $\sigma_{\text{niño}}$. Here we use physics parameter ensembles, in which error compensation was eliminated by perturbing model parameters, to explore relationships between mean climate and variability. With four such ensembles we find a strong relationship between $\sigma_{\text{niño}}$ and the mean precipitation over the eastern equatorial Pacific ($\bar{P}_{\text{niño}}$). This involves a two-way interaction, in which the wetter mean state with greater $\bar{P}_{\text{niño}}$ acts to increase the ENSO amplitude by strengthening positive coupled feedbacks. Such a relationship is also identified in 11 single-model historical climate simulations in the Coupled Model Intercomparison Project phase 5 despite mean precipitation biases apparently masking the relationship in the multi-model ensemble (MME). Taking changes in $\sigma_{\text{niño}}$ and $\bar{P}_{\text{niño}}$ between pre-industrial and recent periods eliminates the bias, and therefore results in a robust $\sigma_{\text{niño}}$–$\bar{P}_{\text{niño}}$ connection in MME, which suggests a 10–15% increase in the ENSO amplitude since pre-industrial era mainly due to changing mean state. However, the $\sigma_{\text{niño}}$–$\bar{P}_{\text{niño}}$ connection is less clear for their future changes, which are still greatly uncertain.
Citation: Watanabe, M., J.-S. Kug, F.-F. Jin, M. Collins, M. Ohba, and A. T. Wittenberg (2012), Uncertainty in the ENSO amplitude change from the past to the future, *Geophys. Res. Lett.*, *39*, L20703, doi:10.1029/2012GL053305.

1. Introduction

[2] With the continuous development of general circulation models (GCMs) over the last few decades, the simulation of ENSO under present climate conditions has become more realistic than before in terms of frequency and spatial structure [*AchutaRao and Sperber*, 2006]. Further, accumulation of recent studies has advanced our understanding a number of processes involved in the dynamics of ENSO [*Collins et al.*, 2010]. Nevertheless, a fundamental ENSO property, namely, amplitude, is still highly model-dependent because of competing feedback processes in different GCMs [*Meehl et al.*, 2007a; *Guilyardi et al.*, 2009a; *Vecchi and Wittenberg*, 2010]. In any member of a multi-model ensemble (MME), there is a potential for compensating errors and structural differences, i.e., differences in parameterization scheme, dynamical core, and resolution, making it difficult to understand the diversity in the ENSO amplitude across the models using a simple metric. It might be, however, possible to attribute changing ENSO amplitude to specific processes in structurally-similar model ensembles in which error compensation may be eliminated by perturbing model parameters.

[3] Recent studies indicate that among the various causes of error and uncertainty in ENSO simulations in GCM ensembles, the atmospheric model serves as an important source of diversity in GCM ensembles [*Guilyardi et al.*, 2004; *Philip et al.*, 2010]. In particular, parameterization schemes for cumulus convection, which affect both positive Bjerknes and negative heat flux feedbacks, greatly influence the ENSO properties [*Neale et al.*, 2008; *Guilyardi et al.*, 2009b; *Watanabe et al.*, 2011; *Kim et al.*, 2011]. Here we use four sets of GCM ensembles in which the atmospheric model parameters have been perturbed (see the next section). The two base models of our perturbed parameter ensembles (PPE) were included in the Coupled Model Intercomparison Project phase 3 (CMIP3) and show great ability to reproduce the present tropical climate [*van Oldenborgh et al.*, 2005; *Meehl et al.*, 2007b]; the other two were developed after CMIP3 and are included in a more recent ensemble of CMIP5 [*Taylor et al.*, 2012], which is partly available as of this writing. In addition to the century-long control experiments using pre-industrial external conditions, we performed experiments involving either abrupt doubling or a 1% increase in the atmospheric CO_2 concentration for each model and parameter set in order to evaluate changes in the ENSO amplitude by global warming. With these experiments, we found that the ENSO amplitude is well measured by the mean rainfall over the eastern equatorial Pacific. This relationship is then applied to CMIP MMEs to discuss the robustness. The evaluation of CMIP5 models is ongoing in parallel with this study, but preliminary results reveal that the diversity of the simulated ENSO property is still large despite the reduced amplitude error over the historical runs in CMIP5 compared to CMIP3 [*Guilyardi et al.*, 2012]. This may not be surprising given the error compensation in MME, but our results suggest that there is a common signal of the ENSO intensification from the pre-industrial era to

[1]Atmosphere and Ocean Research Institute, University of Tokyo, Kashiwa, Japan.
[2]Korea Institute of Ocean Science and Technology, Ansan, South Korea.
[3]Department of Meteorology, University of Hawaii at Manoa, Honolulu, Hawaii, USA.
[4]College of Engineering Mathematics and Physical Sciences, University of Exeter, Exeter, UK.
[5]Hadley Centre for Climate Prediction and Research, Met Office, Exeter, UK.
[6]Central Research Institute of Electric Power Industry, Abiko, Japan.
[7]NOAA Geophysical Fluid Dynamics Laboratory, Princeton, New Jersey, USA.

Corresponding author: M. Watanabe, Atmosphere and Ocean Research Institute, University of Tokyo, Kashiwa, Chiba 277-8568, Japan. (hiro@aori.u-tokyo.ac.jp)

0094-8276/12/2012GL053305

present, which can be interpreted in terms of the mean state change.

2. Model Ensembles

[4] We used the following perturbed parameter ensembles. An ensemble based on the third version of the Hadley Centre climate model (HadCM3) had 17 members, in which 33 atmospheric model parameters were perturbed [*Toniazzo et al.*, 2008]. In each model, a set of pre-industrial control and 1% CO_2 increasing runs was performed for 150 years. The other three models, the fifth version of the Model for Interdisciplinary Research on Climate (MIROC5) [*Watanabe et al.*, 2011], the Geophysical Fluid Dynamics Laboratory coupled model version 2.1 (GFDL CM2.1) [*Kim et al.*, 2011], and the fourth version of the Community Climate System Model (CCSM4) [*Gent et al.*, 2011], each employ a single-parameter ensemble, in which one parameter controlling the cumulus entrainment process is varied among the 4, 5, and 7 members, respectively. Besides control simulations for 100 years using these models, doubled CO_2 experiments were carried out for the same periods.

[5] It is cautioned that different types of the ensembles, i.e. multi-model and parameter ensembles, should not be treated equally because they represent different kinds of uncertainty. Therefore, we did not merge the parameter ensembles with the CMIP MMEs. The combined multi-model statistics are generated by prescribing the sample size for each model as $N = 4$ and repeating the calculation 500 times with randomly selected samples from three models with larger samples. All the model fields have been re-gridded to a regular 2.5° × 2.5° grid before the analysis. The ENSO amplitude ($\sigma_{\text{niño}}$) is defined by the std dev of monthly, linearly de-trended Niño 3 sea surface temperature (SST) anomalies for each period. Since the de-trending is crucial for evaluating $\sigma_{\text{niño}}$ especially in the CMIP MMEs and the HadCM3 parameter ensemble, we have also tested a 1–20 year bandpass filter when calculating $\sigma_{\text{niño}}$, which did not change the conclusions.

[6] We also use CMIP3 and CMIP5 MMEs, consisting of 24 and 18 models, respectively (see *Meehl et al.* [2007b] for CMIP3 models and Table S1 in Text S1 of the auxiliary material for CMIP5 models and experiments).[1] Monthly mean SST and precipitation fields for 1940–1999 are obtained from the 20th century simulations of CMIP3 and CMIP5, and also those fields for 2040–2099 from the Representative Concentration Pathway (RCP) 4.5 scenario experiments and for the entire period from the pre-industrial control experiments of CMIP5.

3. Results

[7] The relevance of parameter ensembles may depend on the ability of the base models in simulating ENSO. When the typical anomalies in SST, precipitation (P), and surface wind stresses during El Niño obtained from the CMIP3 MME and our parameter ensemble are compared with observations, both ensembles reproduce the observed features of El Niño (see Figure S1 in Text S1 of the auxiliary material). The root-mean-square errors of the ENSO-related P and zonal stress (τ_x) anomalies indicate that our ensemble

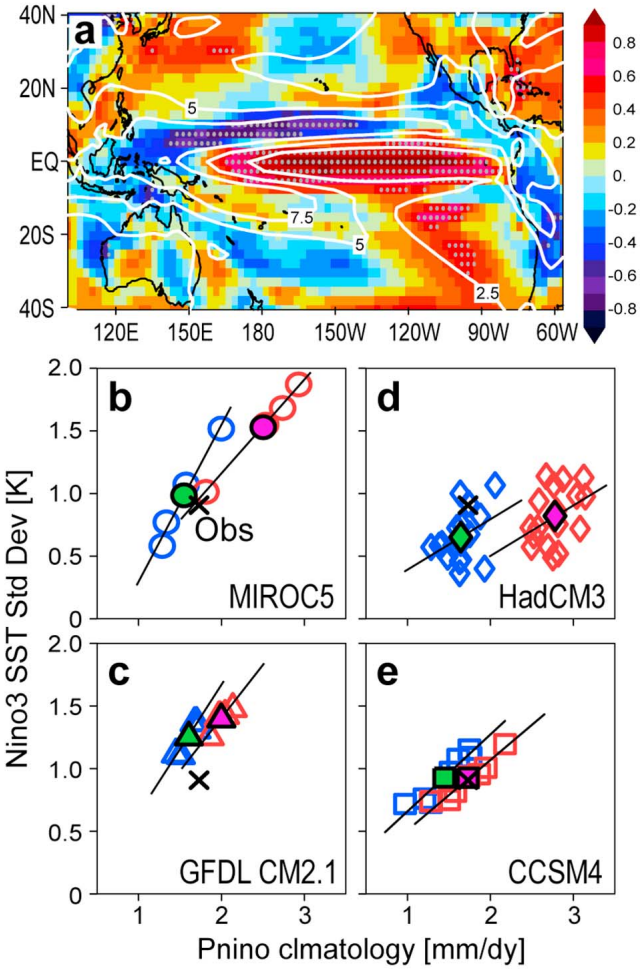

Figure 1. Relationship between ENSO amplitude and mean state in combined parameter ensemble. (a) Correlation of the annual-mean precipitation climatology with the standard deviation of the Niño 3 SST anomalies ($\sigma_{\text{niño}}$) in the control experiments, imposed on the ensemble-mean precipitation climatology (contour, interval of 2.5 mm dy^{-1}). The 95% statistical significance is denoted by dots. (b–e) Scatter diagram of $\sigma_{\text{niño}}$ against the climatological precipitation over the Niño 3 region ($\bar{P}_{\text{niño}}$) in each of the parameter ensembles. The '×' mark indicates the observational estimate for the late 20th century [*Xie and Arkin*, 1997; *Rayner et al.*, 2003]. The blue and red symbols represent the values in the control and increased CO_2 experiments, respectively. The regression slope and the ensemble average are indicated by straight line and a filled symbol for each set of the experiments.

can simulate El Niño and the associated atmospheric response at least as realistically as the CMIP3 MME.

[8] It is likely that the ENSO characteristics are controlled to some extent by the mean atmosphere-ocean state in the tropical Pacific [e.g., *An et al.*, 2008]. To elucidate the details of the ENSO amplitude change across the members, we examine the relationship between the ENSO amplitude as measured by $\sigma_{\text{niño}}$ and the annual-mean precipitation climatology ($\bar{P}$) in the control integrations of our parameter ensembles. By equally weighting the four models, a multi-model mean property of the correlation between $\sigma_{\text{niño}}$ and $\bar{P}$ is obtained (Figure 1a). A significant positive correlation is

[1]Auxiliary materials are available in the HTML. doi:10.1029/2012GL053305.

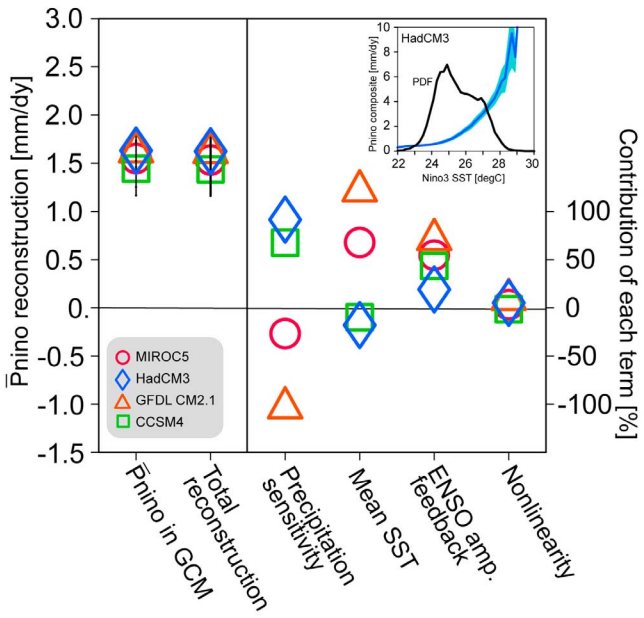

Figure 2. Reconstruction of $\bar{P}_{\text{niño}}$ in the combined PPEs, following equations (1) and (2). The full reconstruction and partial contributions to the diversity in $\bar{P}_{\text{niño}}$ by each of the four terms in equation (2), i.e., changes in the precipitation sensitivity and mean SST, ENSO amplitude feedback, and nonlinearity [cf. *Watanabe and Wittenberg*, 2012], are shown for each parameter ensemble. The diversity in $\bar{P}_{\text{niño}}$ and its reconstruction is presented by the std dev in the ensembles (black vertical lines). Inset panel shows an example of the PDF for the Niño 3 SST (black) and the precipitation composite sorted by the PDF (blue with shading for the error range) calculated with HadCM3 data.

found over the central-eastern equatorial Pacific where $\bar{P}$ is less than 2.5 mm dy^{-1}, surrounded by a negative correlation over the western Pacific and the off-equatorial regions. This implies that the ENSO tends to be stronger in models having a wetter mean condition over the equatorial cold tongue. The above relationship is identified in each parameter ensemble but not in CMIP3 and CMIP5 MMEs (Figure S2 in Text S1 of the auxiliary material).

[9] The scatter diagram between $\sigma_{\text{niño}}$ and $\bar{P}$ over the Niño 3 region ($\bar{P}_{\text{niño}}$) for each model provides further details (Figures 1b–1e). In the pre-industrial control experiments (blue symbols), $\bar{P}_{\text{niño}}$ is 1–2 mm dy^{-1}, which includes the observation ('×' mark), with $\sigma_{\text{niño}}$ varying from 0.3 to 1.5 K. All the ensembles exhibit a positive correlation between $\sigma_{\text{niño}}$ and $\bar{P}_{\text{niño}}$, whereas the mean values and the regression slope are different from each other. The worst linear fitting in HadCM3 may be attributed to the multiple parameters being systematically perturbed and the use of flux-adjustments to prevent model drifts [*Toniazzo et al.*, 2008]. The $\sigma_{\text{niño}}$–$\bar{P}_{\text{niño}}$ relationship in the doubled CO_2 and 1% increased CO_2 experiments (red symbols) is discussed later.

[10] In two of the four models (MIROC5 and GFDL CM2.1), the mechanisms of ENSO intensification with increased $\bar{P}_{\text{niño}}$ in the control runs have been clarified [*Watanabe et al.*, 2011; *Kim et al.*, 2011] (see also Figure S3 in Text S1 of the auxiliary material). When the mean atmosphere becomes wet over the cold tongue, it allows an ENSO-induced precipitation anomaly to occur there, causing the τ_x response to the ENSO-related SST anomaly to shift eastward. The zonal shift in τ_x results in a stronger response in the eastern Pacific thermocline and a larger covariance between the anomalous zonal current and SST, which strengthens the El Niño growth [*Kang and Kug*, 2002]. These processes, corresponding to enhanced thermocline and zonal advective feedbacks [*Collins et al.*, 2010], together with a stronger atmospheric noise forcing, boost ENSO amplitude in a wetter atmospheric mean state [*Kug et al.*, 2008]. Therefore, $\bar{P}_{\text{niño}}$ provides an indicator of the efficacy of several feedback processes associated with the wind stress anomalies.

[11] It is often argued that the ENSO cycle interacts with the mean state in the tropical Pacific [*Guilyardi*, 2006; *Choi et al.*, 2009]. This suggests an alternative possibility in the interpretation of the $\sigma_{\text{niño}}$–$\bar{P}_{\text{niño}}$ relationship identified in Figure 1; stronger ENSO in a model works to increase $\bar{P}_{\text{niño}}$ due to an asymmetry in the precipitation response to the ENSO phase (i.e., P can increase to warmer SST but cannot decrease much to colder SST). This possibility can be examined by using the so-called probability density function (PDF) method for reconstructing $\bar{P}$ [*Watanabe and Wittenberg*, 2012].

$$\bar{P}_{\text{niño}} = \int f(T)C(T)dT, \tag{1}$$

where T is the Niño 3 SST, $f(T)$ is the PDF of T, and $C(T)$ is the composite of the Niño 3 P with respect to T (see inset in Figure 2). Suppose (1) applied to the respective parameter ensemble, the mean precipitation can be expressed with four terms by dividing each quantity into a reference value $(\,)_0$ and the deviation from the reference $(\,)'$.

$$\begin{aligned}\bar{P}_{\text{niño}} - \bar{P}_0 &= \int f' C_0(T)dT + \int f_0 C'(T)dT + \int f' C'(T)dT \\ &= \int \left(f - \hat{f}\right) C_0(T)dT + \int \left(\hat{f} - f_0\right) C_0(T)dT \\ &\quad + \int f_0 C'(T)dT + \int f' C'(T)dT,\end{aligned} \tag{2}$$

where the lhs of (2) indicates the mean precipitation excess in each member. $C_0(T)$ is simply obtained from the ensemble average, while f_0 is calculated by averaging f after the mean position is shifted to each other so that it ensures a plausible mean shape. Since f' consists not only of the difference in the ENSO property but of the difference in mean SST, it is further divided by introducing a virtual PDF, $\hat{f}$, which has the same shape as f_0 except that the mean position follows f. The first term on the rhs of the second equation represents the varying PDF width due to the ENSO amplitude change, and is referred to as the ENSO amplitude feedback. The second term is the effect of mean SST change, while the third term represents the different sensitivity of P to the underlying SST. The last term accounts for nonlinearity between f and $C(T)$, which is much smaller than the other terms. The ENSO feedback to the mean state may also occur via an asymmetry between El Niño and La Niña [*An and Jin*, 2004], acting to increase the mean SST, which is implicitly included in the second term.

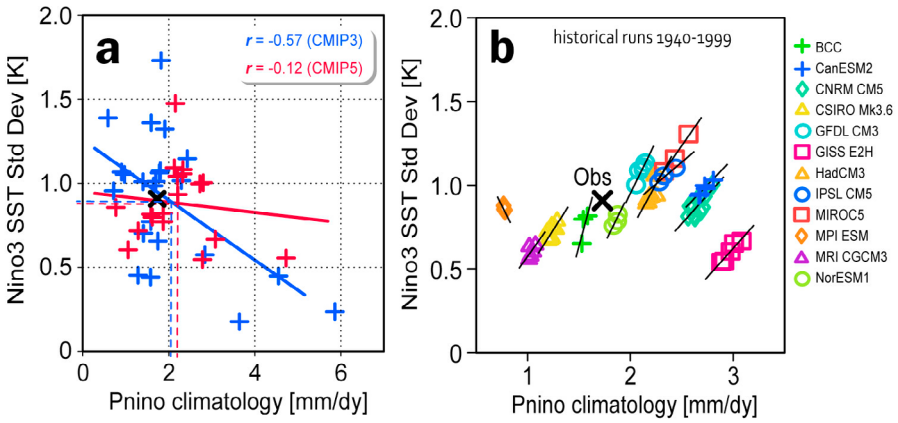

Figure 3. Relationship between ENSO amplitude and mean precipitation in multi-model ensembles, represented as the scatter diagram of $\sigma_{\text{niño}}$ against $\bar{P}_{\text{niño}}$. (a) Estimates for 1940–1999 in the CMIP3 and CMIP5 models (blue and red symbols, respectively), with the ensemble means and the regression slopes indicated by the dashed and solid lines, and (b) each of the ensemble historical experiments for 1940–1999 in CMIP5 (only for models with more than three members). The respective regression slopes and the observational estimate are indicated as in Figures 1b–1e.

[12] When we apply the PDF method to each of the four parameter ensembles, the reconstruction of (1) works by definition in reproducing $\bar{P}_{\text{niño}}$ (Figure 2). The relative contribution of four terms in (2) to the diversity in $\bar{P}_{\text{niño}}$ can be quantified by calculating the linear regression coefficient of each term against the reconstructed mean precipitation. Plotting these values for each parameter ensemble indicates that the diversity in $\bar{P}_{\text{niño}}$ among different members arises from all the terms except for nonlinearity (Figure 2). The differences in the sensitivity of precipitation to SST dominate in HadCM3 and CCSM4, whereas the mean SST effect greatly works to increase $\bar{P}_{\text{niño}}$ in MIROC5 and GFDL CM2.1. The ENSO amplitude feedback to the mean rainfall is positive in all the models and is not negligible; it accounts for about 40% on average. Thus, the $\sigma_{\text{niño}}$–$\bar{P}_{\text{niño}}$ relationship identified in the parameter ensembles involves a two-way coupling between ENSO and the mean state, in which the mean state control of ENSO is slightly greater than the ENSO rectification to the mean state.

[13] Unlike our combined parameter ensemble, the CMIP MMEs show neither a significant correlation between $\sigma_{\text{niño}}$ and $\bar{P}$ (Figure S2 in Text S1 of the auxiliary material) nor a systematic tendency for a future ENSO amplitude change. The scatter diagram of $\sigma_{\text{niño}}$ against $\bar{P}_{\text{niño}}$ for the latter half of the 20th century, 1940–1999, obtained from the historical experiments, appears to be very different from our parameter ensemble (Figure 3a). For the recent 60 years, $\bar{P}_{\text{niño}}$ contains large errors compared with Figures 1b–1e, and the ENSO amplitude is even negatively correlated with $\bar{P}_{\text{niño}}$ in the ensemble, which remains the same in the 21st century (figure not shown).

[14] In addition to a large bias in $\bar{P}_{\text{niño}}$ in the CMIP ensembles, error compensation occurring differently in different models may mask the subtle dependence of $\sigma_{\text{niño}}$ on $\bar{P}_{\text{niño}}$. However, we may still see the relationship akin to Figures 1b–1e in MME if it were not the single-member ensemble. Fortunately, ensembles of the historical runs, in which different initial conditions have been adopted, are available for some of the CMIP5 models. The plot of $\sigma_{\text{niño}}$ and $\bar{P}_{\text{niño}}$ for the above ensemble indeed shows that 11 among 12 models reveal a positive relationship within the respective model (Figure 3b). While the ensemble size and the spread across members are small, the commonly found positive correlation, 0.84 on average, supports robustness of the $\sigma_{\text{niño}}$–$\bar{P}_{\text{niño}}$ relationship. In the absence of changes in model parameters or the external radiative forcing, the ENSO amplitude feedback dominates the other terms in (2) (Figure S4 in Text S1 of the auxiliary material).

[15] The above results not only provide a useful metric that measures the simulated ENSO amplitude but also can be used to explain historical changes in the ENSO intensity. To reduce the sampling noise due to internal variability, we take differences between 1940–1999 and an entire period of the pre-industrial experiment performed with the 1850 external forcing in each model. The change in $\bar{P}$ from the pre-industrial to recent periods, denoted as $\Delta\bar{P}$, is characterized by increase in the tropics and high latitudes while decrease in the subtropics (Figure S5a in Text S1 of the auxiliary material). The value of $\Delta\bar{P}_{\text{niño}}$ is different among models, but is clearly related with the change in $\sigma_{\text{niño}}$, $\Delta\sigma_{\text{niño}}$ (Figure 4a). While $\Delta\sigma_{\text{niño}}$ appears insensitive to $\Delta\bar{P}_{\text{niño}}$ in a few models (INM-CM4, MRI-CGCM3, and NorESM1-M) that show slight decrease in precipitation, the overall relationship in MME is linear with the correlation coefficient of 0.91. The relative contribution of the ENSO-mean state feedbacks examined following (2) was different from Figure 2 and Figure S4 in Text S1 of the auxiliary material, i.e., the weak ENSO amplitude feedback except for limited models showing strong ENSO. The increase in mean SST works to increase $\bar{P}_{\text{niño}}$, which is partly cancelled by the changing precipitation sensitivity (Figure S6 in Text S1 of the auxiliary material). This dominant effect of the mean SST increase for $\Delta\bar{P}_{\text{niño}}$ is also seen in the increased CO_2 experiments of our parameter ensembles. While the magnitude and pattern of $\Delta\bar{P}$ cannot be verified due to lack of the long-term precipitation measurements [*Xie and Arkin*, 1997], there are observed SST data for more than a century [*Rayner et al.*, 2003; *Kaplan et al.*, 1998], which indicate an increase

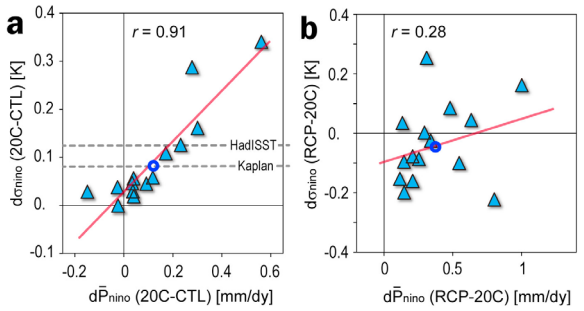

Figure 4. The $\sigma_{niño}$–$\bar{P}_{niño}$ relationship between different eras of the CMIP5 MME. (a) The change in $\sigma_{niño}$ and $\bar{P}_{niño}$ from the pre-industrial (1850 condition) to 1940–1999 periods, and (b) the change from 1940–1999 to 2040–2099 periods, the latter derived from the RCP4.5 experiments. The MME averages are indicated by blue circles. The regression line and the correlation coefficients are also shown. The dashed lines in Figure 4a indicate differences in $\sigma_{niño}$ between 1871–1930 and 1940–1999 estimated from two observational SST data sets [*Rayner et al.*, 2003; *Kaplan et al.*, 1998].

of $\sigma_{niño}$ by 10–15% between 1871–1930 and 1940–1999 periods [*Kang et al.*, 2006] (also Figure 4a). With the limited SST measurements before the World War II, which were used to re-construct the global map, $\sigma_{niño}$ for 1871–1930 is less reliable than that for 1940–1999. Yet, the strong $\Delta\sigma_{niño}$–$\Delta\bar{P}_{niño}$ relationship in the CMIP5 MME, which also gives the ensemble-mean estimate of $\Delta\sigma_{niño}$ within the observational estimates, supports that the increased ENSO variance since the pre-industrial era is physically relevant. However, the natural amplitude modulation of the ENSO activity is considerably large [*Wittenberg*, 2009], implying that the signal-to-noise ratio for the past $\Delta\sigma_{niño}$ should be carefully evaluated.

4. Discussion on Future Changes in ENSO Amplitude

[16] Given that future changes in the ENSO amplitude are not yet conclusive with CMIP3 MME [*Meehl et al.*, 2007a], a question of whether the $\sigma_{niño}$–$\bar{P}_{niño}$ relationship can be used to explain the diversity in the changes in future ENSO amplitude is of great concern. Some common signals of climate change in the tropical Pacific mean state in global warming experiments, such as the weakening of the Walker circulation [*Vecchi et al.*, 2006] and an increase in the equatorial Pacific SST [*Meehl et al.*, 2007a], apparently act to increase $\bar{P}_{niño}$. In the doubled CO_2 and 1% increased CO_2 experiments of our parameter ensembles, $\bar{P}_{niño}$ was shifted toward larger values with little change in the slope of $\partial\sigma_{niño}/\partial\bar{P}_{niño}$ (Figures 1b–1e). In addition to all but one of the ensemble-mean values showing positive changes in $\sigma_{niño}$ as well, most of the individual realizations—all members in MIROC5 and HadCM3, 4 among 5 in GFDL CM2.1, and 3 among 7 in CCSM4— show the same tendency. In HadCM3, a systematic positive shift is also observed in $\bar{P}_{niño}$, which probably arises from transient simulation that tends to amplify the precipitation response. These results suggest an amplification of ENSO in a warmed climate, consistent with some of the GCM studies [*Yeh et al.*, 2006; *Cherchi et al.*, 2008; *Park et al.*, 2009]. However, this idea is not strongly supported by the future scenario experiments in CMIP5 despite a common change of the positive $\Delta\bar{P}_{niño}$ between 1940–1999 and 2040–2099 (Figure 4b). This may not be surprising given coupled feedback processes acting differently to the El Niño growth in a changing climate [*Collins et al.*, 2010], but the similarity in the past and future $\Delta\bar{P}$ patterns is somewhat puzzling (Figure S5b in Text S1 of the auxiliary material). One possibility is that, in a warmed climate, there is another model-dependent suppression mechanism for ENSO, which emerges more slowly than the positive coupled feedback represented by the $\sigma_{niño}$–$\bar{P}_{niño}$ relationship. A deeper analysis for the mechanism of the ENSO amplitude control in CMIP5 experiments is expected to unravel why the ENSO amplitude change in a warmer climate is so uncertain.

[17] **Acknowledgments.** We thank E. Guilyardi, S. Power, J. N. Brown, and an anonymous reviewer for useful comments. We also acknowledge M. Arai, N. Hirota and Y.-S. Jang for the data processing. MW was supported by the Innovative Program of Climate Change Projection for the 21st Century from MEXT, Japan, the Mitsui Environment Fund C-042. FFJ was supported by, NSF ATM 1034439, NOAA NA10OAR4310200, and DOE DESC0005110. JSK was supported by the Korea Meteorological Administration Research and Development Program under grant CATER 2012-3042.

[18] The Editor thanks Jaci Brown and an anonymous reviewer for assistance evaluating this manuscript.

References

AchutaRao, K., and K. Sperber (2006), ENSO simulations in coupled ocean-atmosphere models: Are the current models better?, *Clim. Dyn.*, *27*, 1–15, doi:10.1007/s00382-006-0119-7.

An, S.-I., and F.-F. Jin (2004), Nonlinearity and asymmetry of ENSO, *J. Clim.*, *17*, 2399–2412, doi:10.1175/1520-0442(2004)017<2399:NAAOE>2.0.CO;2.

An, S.-I., J.-S. Kug, Y.-G. Ham, and I. S. Kang (2008), Successive modulation of ENSO to the future greenhouse warming, *J. Clim.*, *21*, 3–21, doi:10.1175/2007JCLI1500.1.

Cherchi, A., S. Masina, and A. Navarra (2008), Impact of extreme CO_2 levels on tropical climate: A CGCM study, *Clim. Dyn.*, *31*, 743–758, doi:10.1007/s00382-008-0414-6.

Choi, J., S.-I. An, B. Dewitte, and W. M. Hsieh (2009), Interactive feedback between the tropical Pacific decadal oscillation and ENSO in a coupled general circulation model, *J. Clim.*, *22*, 6597–6611, doi:10.1175/2009JCLI2782.1.

Collins, M., et al. (2010), The impact of global warming on the tropical Pacific Ocean and El Niño, *Nat. Geosci.*, *3*, 391–397, doi:10.1038/ngeo868.

Gent, P. R., et al. (2011), The community climate system model version 4, *J. Clim.*, *24*, 4973–4991, doi:10.1175/2011JCLI4083.1.

Guilyardi, E. (2006), El Niño–mean state–seasonal cycle interactions in a multi-model ensemble, *Clim. Dyn.*, *26*, 329–348, doi:10.1007/s00382-005-0084-6.

Guilyardi, E., et al. (2004), Representing El Niño in coupled ocean–atmosphere GCMs: The role of the atmospheric component, *J. Clim.*, *17*, 4623–4629, doi:10.1175/JCLI-3260.1.

Guilyardi, E., et al. (2009a), Understanding El Niño in ocean-atmosphere general circulation models: Progress and challenges, *Bull. Am. Meteorol. Soc.*, *90*, 325–340, doi:10.1175/2008BAMS2387.1.

Guilyardi, E., et al. (2009b), Atmospheric feedbacks during ENSO in a coupled GCM with a modified atmospheric convection scheme, *J. Clim.*, *22*, 5698–5718, doi:10.1175/2009JCLI2815.1.

Guilyardi, E., et al. (2012), A first look at ENSO in CMIP5, *CLIVAR Exch.*, *17*, 29–32.

Kang, I.-S., and J.-S. Kug (2002), El Niño and La Niña sea surface temperature anomalies: Asymmetry characteristics associated with their wind stress anomalies, *J. Geophys. Res.*, *107*(D19), 4372, doi:10.1029/2001JD000393.

Kang, I.-S., E. K. Jin, and K.-H. An (2006), Secular increase of seasonal predictability for the 20th century, *Geophys. Res. Lett.*, *33*, L02703, doi:10.1029/2005GL024499.

Kaplan, A., M. A. Cane, Y. Kushnir, A. C. Clement, M. B. Blumenthal, and B. Rajagopalan (1998), Analyses of global sea surface temperature 1856–1991, *J. Geophys. Res.*, *103*, 18,567–18,589, doi:10.1029/97JC01736.

Kim, D., Y.-S. Jang, D.-H. Kim, Y.-H. Kim, M. Watanabe, F.-F. Jin, and J.-S. Kug (2011), ENSO sensitivity to cumulus entrainment in a coupled GCM, *J. Geophys. Res.*, *116*, D22112, doi:10.1029/2011JD016526.

Kug, J.-S., F.-F. Jin, K. P. Sooraj, and I.-S. Kang (2008), State-dependent atmospheric noise associated with ENSO, *Geophys. Res. Lett.*, *35*, L05701, doi:10.1029/2007GL032017.

Meehl, G. A., et al. (2007a), Global climate projections, in *Climate Change 2007: The Physical Science Basis: Contribution of Working Group I to the Fourth Assessment Report of the Intergovernmental Panel on Climate Change*, edited by S. Solomon et al., pp. 747–845, Cambridge Univ. Press, New York.

Meehl, G. A., et al. (2007b), The WCRP CMIP3 multimodel dataset: A new era in climate change research, *Bull. Am. Meteorol. Soc.*, *88*, 1383–1394, doi:10.1175/BAMS-88-9-1383.

Neale, R. B., J. H. Richter, and M. Jochum (2008), The impact of convection on ENSO: From a delayed oscillator to a series of events, *J. Clim.*, *21*, 5904–5924, doi:10.1175/2008JCLI2244.1.

Park, W., et al. (2009), Tropical Pacific climate and its response to global warming in the Kiel climate model, *J. Clim.*, *22*, 71–92, doi:10.1175/2008JCLI2261.1.

Philip, S. Y., M. Collins, G. J. van Oldenborgh, and B. J. J. M. van den Hurk (2010), The role of atmosphere and ocean physical processes in ENSO in a perturbed physics coupled climate model, *Ocean Sci.*, *6*, 441–459, doi:10.5194/os-6-441-2010.

Rayner, N. A., D. E. Parker, E. B. Horton, C. K. Folland, L. V. Alexander, D. P. Rowell, E. C. Kent, and A. Kaplan (2003), Global analyses of sea surface temperature, sea ice, and night marine air temperature since the late nineteenth century, *J. Geophys. Res.*, *108*(D14), 4407, doi:10.1029/2002JD002670.

Taylor, K. E., R. J. Stouffer, and G. A. Meehl (2012), An overview of CMIP5 and the experiment design, *Bull. Am. Meteorol. Soc.*, *93*, 485–498, doi:10.1175/BAMS-D-11-00094.1.

Toniazzo, T., M. Collins, and J. Brown (2008), The variation of ENSO characteristics associated with atmospheric parameter perturbations in a coupled model, *Clim. Dyn.*, *30*, 643–656, doi:10.1007/s00382-007-0313-2.

van Oldenborgh, G. J., S. Philip, and M. Collins (2005), El Niño in a changing climate: A multi-model study, *Ocean Sci.*, *2*, 267–298, doi:10.5194/osd-2-267-2005.

Vecchi, G. A., and A. T. Wittenberg (2010), El Niño and our future climate: Where do we stand? *Wiley Interdisciplinary Rev. Clim. Change*, *1*, 260–270, doi:10.1002/wcc.33.

Vecchi G. A., et al. (2006), Weakening of tropical Pacific atmospheric circulation due to anthropogenic forcing, *Nature*, *441*, 73–76, doi:10.1038/nature04744.

Watanabe, M., and A. T. Wittenberg (2012), A method for disentangling El Niño-mean state interaction, *Geophys. Res. Lett.*, *39*, L14702, doi:10.1029/2012GL052013.

Watanabe, M., M. Chikira, Y. Imada, and M. Kimoto (2011), Convective control of ENSO simulated in MIROC5, *J. Clim.*, *24*, 543–562, doi:10.1175/2010JCLI3878.1.

Wittenberg, A. T. (2009), Are historical records sufficient to constrain ENSO simulations?, *Geophys. Res. Lett.*, *36*, L12702, doi:10.1029/2009GL038710.

Xie, P., and P. A. Arkin (1997), Global precipitation: A 17-year monthly analysis based on gauge observations, satellite estimates, and numerical model outputs, *Bull. Am. Meteorol. Soc.*, *78*, 2539–2558, doi:10.1175/1520-0477(1997)078<2539:GPAYMA>2.0.CO;2.

Yeh, S.-W., Y. G. Park, and B. P. Kirtman (2006), ENSO amplitude changes in climate change commitment to atmospheric CO_2 doubling, *Geophys. Res. Lett.*, *33*, L13711, doi:10.1029/2005GL025653.